The development of surface contour changes during interdiffusion in silver/gold alloy diffusion couples

1995 J. Phys.: Condens. Matter 7 2655

(http://iopscience.iop.org/0953-8984/7/14/006)

J. Phys.: Condens. Matter 7 (1995) 2655–2666. Printed in the UK

The development of surface contour changes during interdiffusion in silver/gold alloy diffusion couples

Reimar Voigt and Volker Ruth

Fachbereich Physik, Universität Oldenburg, D-26111 Oldenburg, Postfach 2503, Germany

Received 24 October 1994, in final form 25 January 1995

Abstract. The development of surface contour changes at about the welding interfaces of silver/gold alloy diffusion couples with various terminal gold concentrations has been investigated for an annealing temperature of 1081 K. The surface profiles were measured at nine different annealing times for each of the employed diffusion couples. The cross-sectional areas of the developing bulge and groove increase proportionally with annealing time, as has already been observed in other systems. The results can be described in terms of reduced growth coefficients. The unexpected decrease of the effects at high silver concentrations could be explained by a model of mass compensation based on plastic deformation.

1. Introduction

In many diffusion systems an observed shift of the Kirkendall interface is associated with a change of the samples' surface contours in the vicinity of the welding interface. Both the longitudinal shift of the Kirkendall interface and the change of the specimen's lateral dimensions are integrated effects of local expansions and contractions of the volume elements of the sample. Together with the formation of pores the local volume dilatations compensate for local divergences of total diffusion fluxes that arise when in multicomponent diffusion systems the components diffuse with different rates [1–3]. Depending on whether the divergence of the total diffusion flux leads to local sub- or supersaturation of vacancy concentrations the volume elements will expand or contract in order to maintain equilibrium vacancy concentration. The swelling and shrinkage of the volume elements is usually believed to proceed via a production and elimination of vacancies at dislocations, grain boundaries, and other vacancy sources and sinks within the material. Also in one-component systems the phenomenon of lateral dimensional changes has been observed in connection with electromigration [4, 5] and thermomigration [6].

The relation of a volume element's expansion and/or contraction in diffusion direction to its total volume change defines the isotropy factor α with the limiting values $\frac{1}{3}$ and 1, where $\alpha = \frac{1}{3}$ corresponds to an ideal isotropic volume change and $\alpha = 1$ to purely axial deformation [4]. It should be noted that the case of ideal anisotropy is assumed when Darken's equations are employed for the determination of intrinsic diffusion coefficients. This case, corresponding to $\alpha = 1$, would imply that only lattice planes perpendicular to the diffusional fluxes are created or eliminated which seems to be rather inconceivable in view of the assumed mechanism of vacancy elimination/creation at dislocations and grain boundaries. Therefore, it is expected that the divergence of the total diffusional fluxes should cause isotropic dimensional changes of all volume elements of the sample if the local volume changes were not constrained by the specimen itself. As has been discussed

0953-8984/95/142655+12$19.50

by several authors [5, 7, 8] the constraints generated by the specimen itself should yield an overall effect of approximately $\alpha = 1$ for 'massive samples' whereas for 'thin samples' the constraints are expected to be diminished leading to an overall effect of $\alpha = \frac{1}{3}$. Huntington and Grone [4] and Penney [5] assumed that during electromigration in thin wires α was $\frac{1}{3}$ at any point within the specimen. In this case of 'thin samples' the lateral dimensional changes should be proportional to the thickness of the specimen. Consequently, from the very observation of lateral dimensional changes *independent* of the sample's thickness during Kirkendall experiments on 'massive samples' one must conclude that in these cases α is a function of the distance from the surface with α being unity at about the axial centre of the specimen and decreasing to $\frac{1}{3}$ only in near-surface regions. Penney [5] has developed a theory for the case of electromigration in thin wires predicting the ratio of longitudinal to lateral dimensional changes to depend on the geometry of the sample as well as on Poisson's ratio ν of the material involved. Since the application of Penney's theory is confined to thin specimens and because of an undetermined parameter b inherent in the theory, one cannot predict the extent of lateral dimensional changes in massive diffusion couples. However, in the current paper a model is proposed according to which contrary to longitudinal volume changes the lateral ones are expected to be constrained. In accordance with the premises of Penney's theory the constraint is expected to increase with the distance from the surface and should depend on the critical shear stress of the respective material at diffusion temperature.

In previous papers the effects of lateral dimensional changes and their dependence on annealing time and temperature have been treated for binary semi-infinite diffusion couples composed of pure gold and silver half-samples [1, 2]. In this communication we report on an investigation of surface contour changes occurring during interdiffusion in silver–gold alloy diffusion couples with different terminal gold concentrations. The measurements are confined to only one annealing temperature, but, instead, the influence of the concentration range on the effects is considered.

2. Experimental procedure

The diffusion experiments were carried out with diffusion couples composed of half-samples with different silver–gold compositions. Beside gold and silver rods with a nominal purity of 99.999%, alloy rods containing 25, 50, and 75 at.% Au had been combined to form the following nine diffusion couples: 100/75, 100/50, 100/25, 75/50, 75/25, 75/0, 50/25, 50/0, and 25/0, where the figures are the terminal gold concentrations of the couples, given in at.%.

For each experiment pieces of about 4 mm length had been cut from two cylindrical rods of different compositions with a diamond saw and the cutting areas were ground and polished. Subsequently, the appropriate pieces were welded for 45 minutes with a pressure of 1.22 N mm^{-2} at a temperature of 1123 K under an argon atmosphere. The welded cylinders had a diameter of 5 mm and were cut along their axes into two semicylinders. The cutting areas were ground and polished and a notch was scratched parallel to the welding interface onto the surface of the slower-diffusing component's side of the couple at a distance of about 600 μm from the welding interface, serving as a fixed reference mark for the measurements. The surface profile of the diffusion couple is determined by moving a diamond tip of a modified roughness tester in the diffusion direction along ten different lines parallel to each other on the sample's surface. For the evaluation the average profile curves are taken. The determination of the surface contour is repeated after each annealing period corresponding to total diffusion times ranging from 100 to 8100 minutes. Before

the onset of diffusion anneal the distance between the welding interface and the scratched reference notch is measured by means of a light microscope. The annealing is carried out under argon atmosphere at a temperature of 1081 K. For a more detailed description of the preparation techniques and the methods of measurement and evaluation we refer to a preceding paper [1].

3. Experimental results

For a discussion of the experimental results it is reasonable to identify the employed concentration ranges by two independent parameters, the difference between the terminal gold concentrations of the sample (given as mole fractions)

$$\Delta N_{Au} = N_{Au}^{+\infty} - N_{Au}^{-\infty} \tag{1}$$

and the mean concentration

$$\bar{N}_{Au} = \frac{N_{Au}^{+\infty} + N_{Au}^{-\infty}}{2}. \tag{2}$$

ΔN_{Au} defines the width and $\bar{N}_{Au}$ the position of the chosen concentration range.

In figures 1(a)–(d) the surface profiles of four diffusion couples with an initial concentration step ΔN_{Au} of 0.25 are given as obtained for nine different annealing times. In figures 2(a) and (b) two sets of surface profiles are given for diffusion systems with $\Delta N_{Au} = 0.75$ whose $\bar{N}_{Au}$ values are identical with those of figures 1(b) and (c), respectively. A comparison of the corresponding profile curves in figures 1 and 2 indicates that the effects are more pronounced for systems with higher initial concentration steps than for those with lower ones at the same $\bar{N}_{Au}$ values. The remaining three sets of profile curves that are evaluated correspond to an initial concentration step ΔN_{Au} of 0.5 and are given in figures 3(a)–(c).

Table 1. Growth coefficients of the bulge, b_b, and the groove, b_g, and their reduced quantities f_b and f_g. Experimental results of Busch and Ruth [1] have been included (No 6). The growth coefficients are given in units of $\mu m^2\ min^{-1}$.

No	$\bar{N}_{Au}$	ΔN_{Au}	b_b	b_g	f_b	f_g	Figure/reference
1	0.125	0.25	0.548	0.089	0.773	0.038	1(a)
2	0.25	0.50	0.994	0.125	1.180	0.081	3(a)
3	0.375	0.25	0.728	0.376	1.027	0.159	1(b)
4	0.375	0.75	1.038	0.158	1.115	0.132	2(a)
5	0.50	0.50	1.243	0.345	1.476	0.224	3(b)
6	0.50	1.00	1.159	0.208	1.159	0.208	[1]
7	0.625	0.25	0.808	0.231	1.140	0.097	1(c)
8	0.625	0.75	1.238	0.454	1.330	0.308	2(b)
9	0.75	0.50	0.516	0.280	0.613	0.182	3(c)
10	0.875	0.25	0.250	0.231	0.353	0.097	1(d)

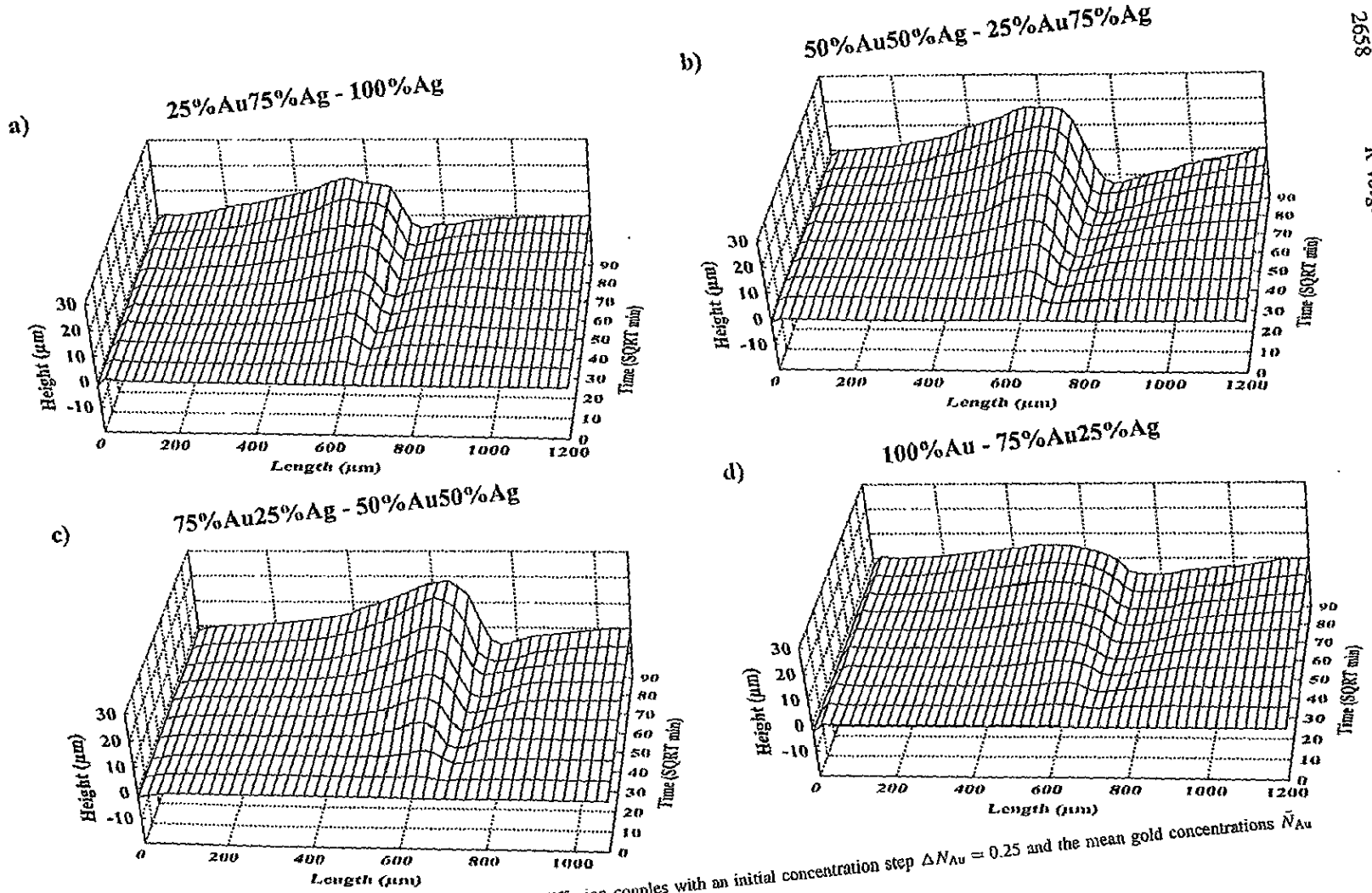

Figure 1. Surface contour changes at 1081 K of Au/Ag alloy diffusion couples with an initial concentration step $\Delta N_{Au} = 0.25$ and the mean gold concentrations $\bar{N}_{Au}$ of (a) 0.125, (b) 0.375, (c) 0.625, and (d) 0.875.

4. Evaluation of experimental results

The already earlier observed time law of the development of surface contour changes [1] is also confirmed for the investigated silver/gold alloy diffusion couples: the cross-sectional areas of the bulge and the groove, $A_b(t)$ and $A_g(t)$, both grow linearly with time [3]

$$A_{b,g}(t) = b_{b,g}t. \tag{3}$$

The slopes b_b and b_g can be determined by regression of a plot of the A_b and A_g values versus annealing time t. The cross-sectional areas are obtained from the measured profile curves. The parameters b_b and b_g are taken as measures for the effects of bulge and groove growth and are listed in table 1. Growth coefficients for a 100/0 diffusion couple (with $\bar{N}_{Au} = 0.50$ and $\Delta N_{Au} = 1.00$) as derived from experimental results that had previously been obtained in our laboratory [1] have been included. For the subsequent evaluation these data are also considered.

The analysis of data is carried out separately for the bulge and the groove zones. For the diffusion couples with an initial concentration step $\Delta N_{Au} = 0.25$ (corresponding to figures 1(a)–(d)) a plot of the slopes b_b versus $\bar{N}_{Au}$ is given in figure 4. The obtained curve has a maximum between $\bar{N}_{Au} = 0.375$ and 0.625. A maximum of the b values at about $\bar{N}_{Au} = 0.5$ is also indicated for the corresponding b values describing the growth of the groove for $\Delta N_{Au} = 0.25$ as well as for the development of the bulge and the groove for diffusion couples with an initial concentration step $\Delta N_{Au} = 0.5$. There is also some evidence that the effects increase with increasing width of the employed concentration range as has already been stated in the preceding section of this paper. Therefore, it seems reasonable to state the empirical equation

$$b(\bar{N}_{Au}, \Delta N_{Au}) = f(\bar{N}_{Au})(\Delta N_{Au})^m \tag{4}$$

defining a reduced growth coefficient f that only depends on $\bar{N}_{Au}$. The fitting parameter m is estimated by minimizing the expression

$$\sum_{i=1}^{3} \left[\frac{b_{i,1}}{(\Delta N_{Au}^{i,1})^m} - \frac{b_{i,2}}{(\Delta N_{Au}^{i,2})^m} \right]^2 \tag{5}$$

where the index i refers to the $\bar{N}_{Au}$ values 0.375, 0.500, and 0.625. For each of these mean concentrations measurements of the slopes b have been carried out for two different concentration widths ΔN_{Au}. The corresponding values for $b_{i,j}$ and $\Delta N_{Au}^{i,j}$ are taken from the experimental results No 3–8 of table 1. The minimizing procedure yields $m = 0.248$ for the growth of the bulge and $m = -0.623$ for the groove. With these values the reduced growth coefficients $f(\bar{N}_{Au})$ are calculated that are listed in columns 5 and 6 of table 1. Plots of f_b and f_g versus $\bar{N}_{Au}$ are given in figures 5 and 6.

5. Discussion and conclusion

The concentration dependences of the reduced growth coefficients f_b and f_g can be presented for each of the corresponding effects by a single curve when the empirical fitting parameters m are employed. There is no analogue to pore formation on the bulge side of the specimen [3] and, consequently, longitudinal and lateral volume expansions on the slower-diffusing

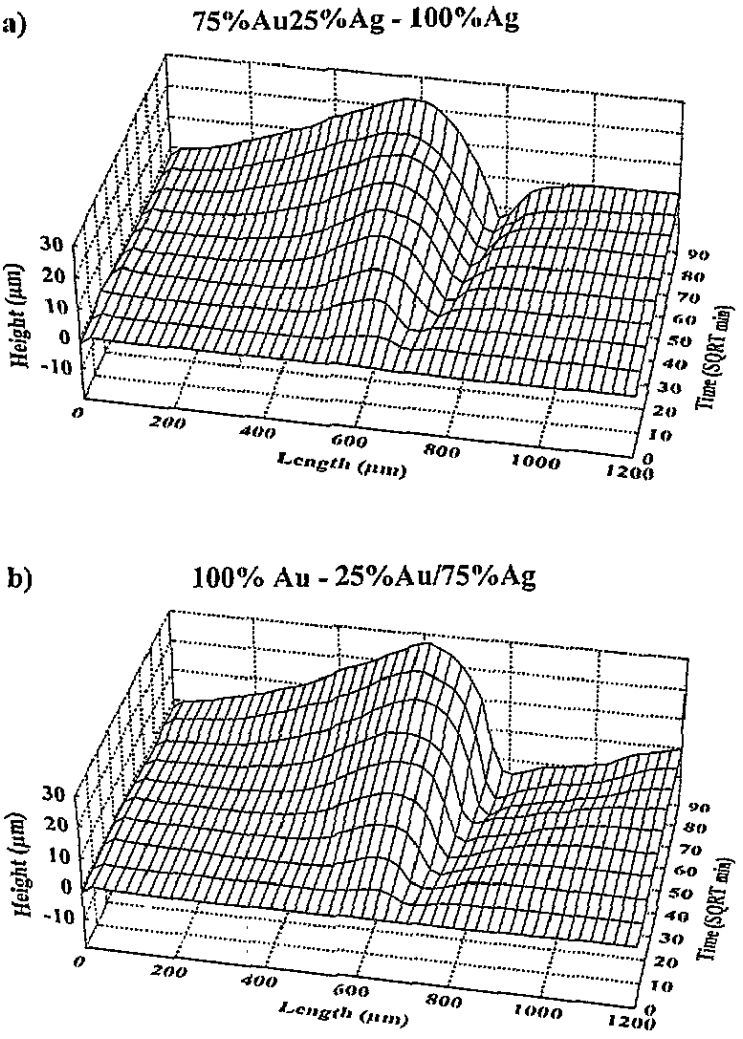

Figure 2. Surface contour changes at 1081 K of Au/Ag alloy diffusion couples with an initial concentration step $\Delta N_{Au} = 0.75$ and the mean gold concentrations $\bar{N}_{Au}$ of (a) 0.375 and (b) 0.625.

component's side of the specimen are usually more pronounced than the corresponding volume contractions on the other side of the diffusion couple. Therefore, it is not surprising that different growth laws (with different m values) govern the bulge and the groove formations.

Both curves, depicted in figures 5 and 6, are characterized by a maximum between 50 and 60 at.% Au. The pronounced decline at both ends of the total concentration range can be explained by a consideration of the processes leading to the Kirkendall shift (longitudinal expansions and contractions) and the bulge and groove formation (lateral expansions and contractions).

The overall process consists of two parts: (i) local changes of particle density due to an imbalance of diffusion rates and (ii) the subsequent—but simultaneously occurring—

a)

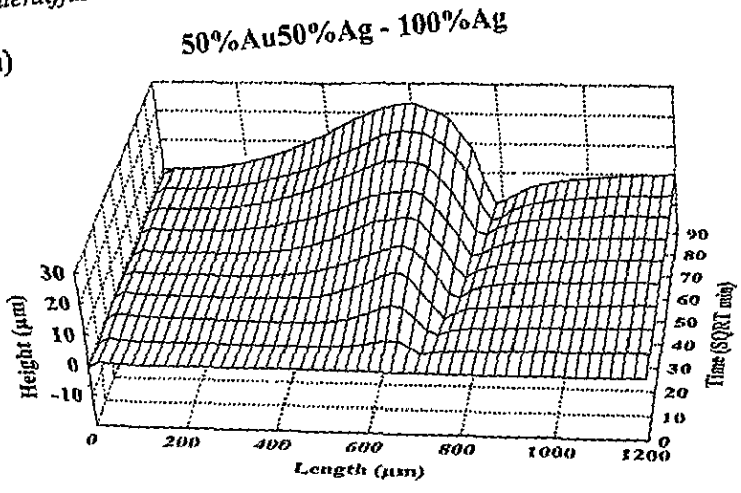

b)

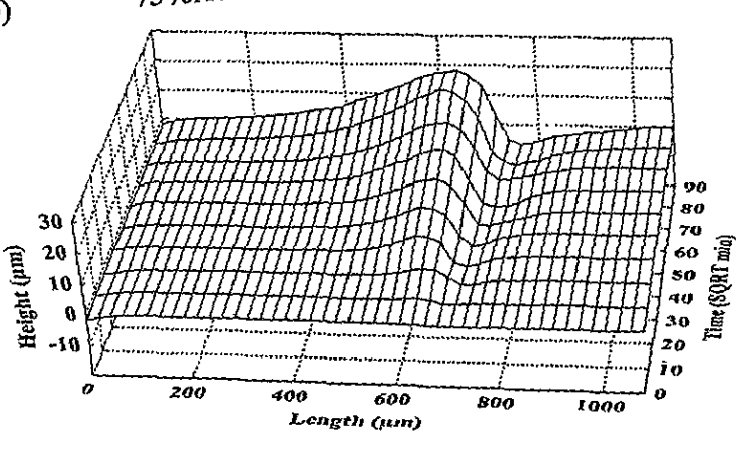

c)

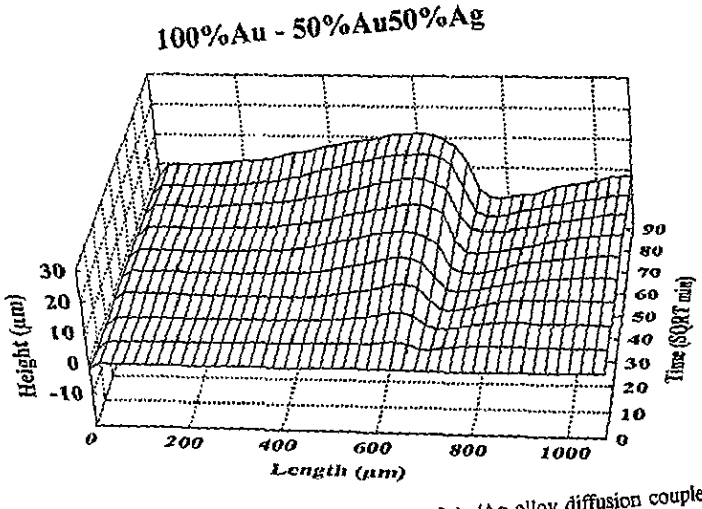

Figure 3. Surface contour changes at 1081 K of Au/Ag alloy diffusion couples with an initial concentration step $\Delta N_{Au} = 0.5$ and the mean gold concentrations $\bar{N}_{Au}$ of (a) 0.25, (b) 0.50, and (c) 0.75.

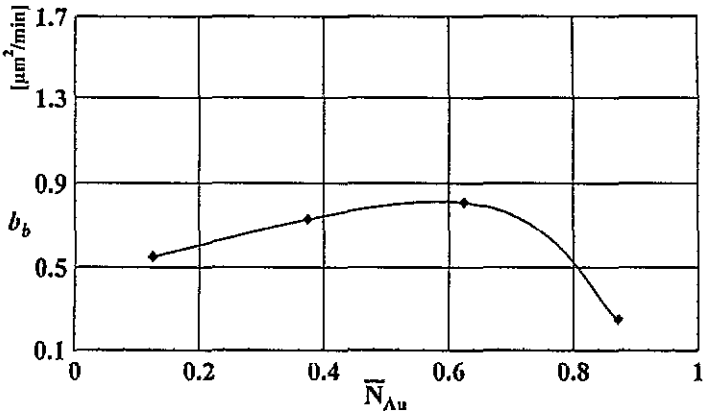

Figure 4. Plot of slopes b_b versus $\bar{N}_{Au}$ for an initial concentration step $\Delta N_{Au} = 0.25$ (corresponding to figures 1(a)–(d))

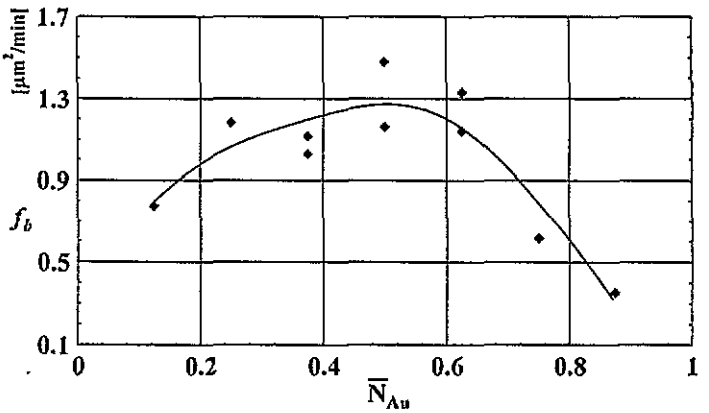

Figure 5. Variation of the reduced growth coefficient f_b of the bulge formation (column 5 of table 1) with the mean gold concentration $\bar{N}_{Au}$.

compensation of the resulting excess concentrations of atoms or vacancies, manifested by longitudinal and lateral volume changes as well as by a formation of pores [3]. The *relative* contributions of these three phenomena to the total required mass compensation are expected to depend upon the specific physical situation prevailing. Here, we confine the discussion to longitudinal and lateral volume changes, the only mass-compensating phenomena, observed on the slower-diffusing component's side of a diffusion couple. It is evident that in cases where the mass-compensational processes (ii) can proceed much faster than the mass-imbalance-initiating process (i) the latter will become rate controlling and the overall effect is expected to attain the composition dependence of the imbalance of diffusion rates. If, however, one of the mass-compensation processes (ii) cannot keep up with the mass-imbalance-initiating process (i) its relative contribution to the total mass compensation will appear to be reduced in favour of the alternative compensational process. In this case, the diffusion-induced generation of excess concentrations of atoms or vacancies is no longer rate controlling for the slower one of the compensational processes and its

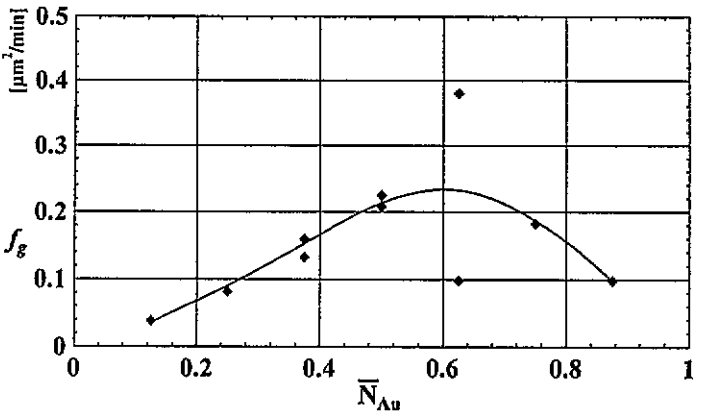

Figure 6. Variation of the reduced growth coefficient f_g of the groove formation (column 6 of table 1) with the mean gold concentration $\bar{N}_{Au}$.

composition dependence may deviate from that of the imbalance of diffusion rates.

For the following discussion it is sufficient to know the tendency of the concentration dependence of imbalance of diffusion rates over the entire concentration range and to compare it with that of our obtained curves, depicted in figures 5 and 6. Therefore, it is justified to confine the consideration to an estimate of the imbalance of diffusion rates in a binary gold/silver diffusion system, $j_m(x,t)$, which can be written as

$$j_m(x,t) = c(x,t)\ (D_{Ag} - D_{Au})_x \left(\frac{\partial N_{Au}}{\partial x}\right)_x \tag{6}$$

with the total particle concentration $c(x,t)$ and the components' individual diffusion coefficients D_{Ag} and D_{Au}. According to Morral this expression can be approximated for the vicinity of the position x_K of the welding interface if some idealizing conditions are fulfilled [9]. For the gold/silver system these assumptions should be fairly well fulfilled and since the pertinent diffusion [10] and thermodynamic data [11] are available for this system, $j_m(x,t)$ at x_K can be estimated for the considered annealing temperature. The calculation yields

$$(D_{Ag} - D_{Au})_{x_K} \left(\frac{\partial N_{Au}}{\partial x}\right)_{x_K} = \tilde{f}^2(\bar{N}_{Au}) \frac{\Delta N_{Au}}{\sqrt{t}} \tag{7}$$

where the function $\tilde{f}(\bar{N}_{Au})$, figure 7, describes the concentration dependence of the mass-imbalance-generating process and should correspond to the reduced growth coefficients f_b and f_g. A comparison of figures 5 and 6 with figure 7 leads to the conclusion that on the gold-rich side of the concentration range the diffusional generation of a mass imbalance is likely to be the rate-controlling process of the bulge and groove formation, since all three curves show the same tendency of concentration dependence at the regime of high gold concentrations. This, however, does obviously not apply for the surface effects observed at silver-rich diffusion couples: whereas the approximated imbalance of diffusion rates continues to increase with decreasing gold concentration, the corresponding f values do decrease. The opposite behaviour of the $f(\bar{N}_{Au})$ and the $\tilde{f}(\bar{N}_{Au})$ curves suggests that at higher silver concentrations not the imbalance-*generating* but the

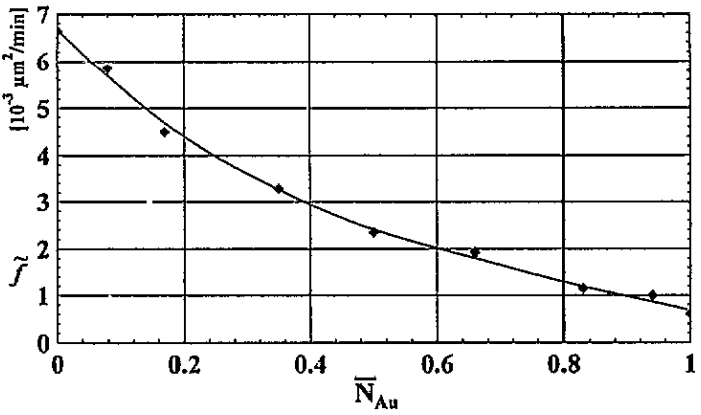

Figure 7. The function $\tilde{f}(\bar{N}_{Au})$ of Eq. (7) as determined according to the Morral approximation [9] employing diffusion [10] and thermodynamical [11] data for 1081 K.

imbalance-*compensating* processes is rate controlling for the specimens' lateral expansions and contractions. Following the preceding argumentation it can be concluded that in silver rich alloys the formation of a bulge and groove zone is retarded, whereas the longitudinal volume changes are not hampered.

The different behaviour of lateral and longitudinal volume changes at high silver concentrations can be explained by a model of mass compensation based on plastic deformation. According to figure 8 the local lateral volume changes' variation in diffusion direction corresponds to a shear of the material normal to the diffusion direction whereas the longitudinal volume changes are not associated with shear. In materials with high yield strength the plastic deformation by shear is expected to be hampered and, consequently, surface contour changes should appear to be reduced in favour of longitudinal volume changes. This model leads to the same consequences as the 'simplified theory of plastic flow' of Penney, who predicts that in thicker electromigration specimens internal constraints should give rise to plastic flow leading to a decrease of lateral dimensional changes [5].

Unfortunately, there are no experimental data concerning the yield strength of silver/gold alloys at elevated temperatures known to the authors. However, there is some evidence that, indeed, the yield strength of silver-rich silver/gold alloys exceeds the yield strength of gold-rich alloys. Measurements of the microhardness of silver/gold alloys in our laboratory employing the Vickers method have revealed that at room temperature the hardness of silver-rich alloys is higher than the hardness of gold-rich ones [12]. Unfortunately, a hot-hardness tester was not available, but assuming only a moderate temperature dependence of the constants A and B in the Westbrook relation [13]

$$H = A\,e^{-BT} \tag{8}$$

(with hardness H in arbitrary units) a similar behaviour could be expected at diffusion temperature. According to Cahoon *et al* the yield strength σ_0 of a material can be related with good precision to the Vickers hardness H_V by

$$\sigma_0 = \frac{H_V}{3}(0.1)^{n-2} \tag{9}$$

where n is a number of about 2.5 [14]. Considering the proportionality between the yield strength and the Vickers hardness expressed by equation (9) and the approximation provided

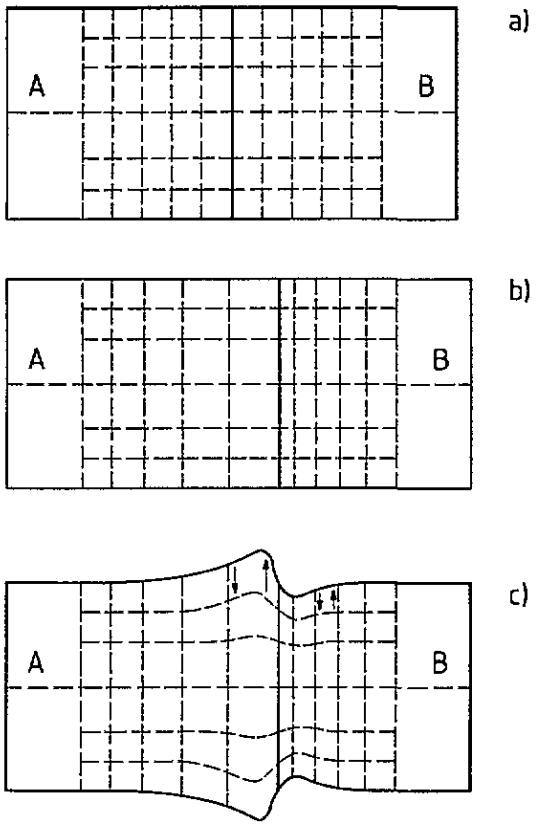

Figure 8. Schematic drawing of an axial section of a diffusion couple with its volume elements: (a) Before onset of diffusion, (b) after diffusion with longitudinal, and (c) with longitudinal and lateral volume changes. Case (c) is associated with a shear of volume elements.

by the Westbrook relation (8) it seems to be justified to conclude from our hardness measurements that also at diffusion temperature silver-rich alloys are characterized by a higher yield strength than gold-rich ones.

Hence, the unexpected decrease of lateral volume changes at silver-rich diffusion couples can be explained by a higher yield strength of silver-rich silver/gold alloys in comparison to gold-rich alloys at the pertinent diffusion temperature.

Acknowledgments

The financial support of this research by the Deutsche Forschungsgemeinschaft (project No Ru 362/7-1) is gratefully acknowledged. We are indebted to DEGUSSA for providing the gold/silver alloy specimens as a generous loan of noble metals.

References

[1] Busch R and Ruth V 1989 *Z. Metallkd.* **80** 238
[2] Busch R and Ruth V 1991 *Acta Metall. Mater.* **39** 1535

[3] Voigt R and Ruth V 1994 *Scr. Metall.* **31** 847
[4] Huntington H B and Grone A R 1961 *J. Phys. Chem. Solids* **20** 76
[5] Penney R V 1964 *J. Phys. Chem. Solids* **25** 225
[6] Feller H G, Wever H and Wilke C 1963 *Z. Naturf.* a **18** 1225
[7] Philibert J 1991 *Atom Movements, Diffusion and Mass Transport in Solids* (Les Ulis: Éditions de Physique) p 334
[8] Wever H 1973 *Elektro- und Thermotransport in Metallen* (Leipzig: Barth) p 132
[9] Morral J E, Son Yoon-Ho and Thompson M S 1988 *Acta Metall.* **36** 1971
[10] Mallard W C, Gardner A B, Bass R F and Slifkin L M 1963 *Phys. Rev.* **129** 617
[11] Hultgren R, Orr R L, Anderson P D and Kelley K K 1963 *Selected Values of Thermodynamic Properties of Metals and Alloys* (New York: Wiley) p 339
[12] Kickstein J 1994 *Studienarbeit* Universität Oldenburg
[13] Westbrook J H 1953 *Trans. Am. Soc. Met.* **45** 221
[14] Cahoon J B, Broughton W H and Kutzak A R 1971 *Metall. Trans.* **2** 1979